Research Article

Investigating the Parameters Affecting the Stability of Superparamagnetic Iron Oxide-Loaded Nanoemulsion Using Artificial Neural Networks

Gholamreza Ahmadi Lakalayeh,[1] Reza Faridi-Majidi,[1] Reza Saber,[1,2] Alireza Partoazar,[1,3] Shahram Ejtemaei Mehr,[3] and Amir Amani[1,4,5]

Abstract. Nanoemulsions are increasingly being investigated for their fascinating capability of loading both hydrophobic and hydrophilic molecules while their stability is still an issue, being affected by various factors. In this study, to evaluate the dominant factors affecting the stability of nanoemulsions, artificial neural networks (ANNs) were implemented. Nanoemulsions of almond oil in water containing oleic acid-coated superparamagnetic iron oxide nanoparticles were prepared using a mixture of Tween 80 and Span 80 as surfactant system and ethanol as a co-surfactant. The ratio of transparency of the samples at 30 min and 7 days after preparation was taken as an indication of the stability of samples. Four independent variables, namely, concentration of nanoparticle, surfactant, oil, and alcohol were investigated to find their relations with the dependent variable (*i.e.*, transparency ratio). Using ANNs modeling, it was concluded that the stability is affected by all variables, with all variables showing reverse effect on the stability beyond an optimum amount.

INTRODUCTION

Nowadays, superparamagnetic iron oxide nanoparticles (SPIONs) have attracted a great deal of attention to be utilized in various medical applications such as drug and gene delivery [1], hyperthermia [2], tissue engineering [1,3], and cellular labeling and cell separation [4], with probably the most interesting use as contrast agents in magnetic resonance imaging (MRI) [5,6].

Following *in vivo* administration of SPIONs, increasing the intracellular iron oxide levels leads to apoptosis and DNA fragmentation [7,8] or can result in oxidative stress and cell damage due to formation of reactive oxygen species leading to cell death [9,10]. Therefore, coating these particles to reduce the possible toxicities may be of high importance in medical applications, as observed in Feridex IV® (Berlex Laboratories, Wayne, New Jersey), a dextran-coated SPION utilized as a MRI contrast agent to image hepatic tissue [11]. Coating systems also commonly affect the stability of colloidal dispersions due to electrostatic and/or steric repulsion forces [12]. They can also reduce biologically non-specific adsorptions, like adsorbing of plasma protein on the surface of nanoparticles (NPs), which may lead to clearance by reticule endothelial system [2]. In order to minimize such effects, many coating polymers (*e.g.*, dextran, polyethylene glycol (PEG), and polyvinyl alcohol (PVA)) have been successfully employed to modify or functionalize NP surface [13].

In addition to the polymers, liposome (magnetosome) and micelles with amphiphilic block copolymers have also been suggested to coat SPIONs in the literature [14,15]. For instance, Yang *et al.* reported synthesized micelles of biodegradable copolymers (PEG-PVA) carrying SPIONs and doxorubicin with high efficacy of the anticancer drug in addition to the potential for use in MRI [16]. In another study, Nasongkla *et al.* have reported micelles of copolymers of MAL-PLG-PLA containing SPIONs and doxorubicin as having targeting agents on the surface of micelles [14]. The only work on SPIONs-loaded nanoemulsions is by Jarzyna *et al.*, reporting selective accumulation of SPIONs in tumor with better quality in MRI images [5]. However, no work so far has detailed the physicochemical properties of such systems (including the stability of the SPIONs-loaded nanoemulsion) as the first step to develop a nanoemulsion-based preparation containing SPIONs.

Reviewing the literature, several studies report the stability of nanoemulsions. Parameters such as zeta potential, molecular structure of co-surfactant [17], ratio of surfactant to co-surfactant [18], molecular structure of oil [19], pH [20], and applied

[1] Department of Medical Nanotechnology, School of Advanced Technologies in Medicine, Tehran University of Medical Sciences, Tehran, Iran.

[2] Nanotechnology Group, Research Center for Science and Technology in Medicine (RCSTIM), Tehran University of Medical Science, Tehran, Iran.

[3] Department of Pharmacology, School of Medicine, Tehran University of Medical Sciences, Tehran, Iran.

[4] Biotechnology Research Center, Tehran University of Medical Sciences, Tehran, Iran.

[5] To whom correspondence should be addressed. (e-mail: aamani@sina.tums.ac.ir)

Table I. The Training and Test Data Set Used in ANN Modeling (*n*=1)

Nanoparticle amount, mg/20 cm³	Oil concentration, %v/v	Surfactant concentration, %v/v	Alcohol concentration, %v/v	Result (TR)	Predicted result (TR)	Result error
1.0	7	18	3.0	0.386	0.459	0.070
1.8	6	18	3.4	0.462	0.577	0.110
0.6	4	20	3.6	0.498	0.538	0.040
0.9	7	16	2.0	0.524	0.543	0.010
1.7	4	18	2.0	0.565	0.752	0.180
0.8	6	20	2.6	0.592	0.620	0.020
0.7	6	15	2.0	0.605	0.558	−0.400
1.2	5	18	3.2	0.614	0.703	0.080
1.2	5	19	3.6	0.615	0.518	−0.090
1.3	4	15	2.7	0.632	0.753	0.120
0.5	6	17	4.0	0.648	0.702	0.050
0.4	5	15	2.0	0.658	0.671	0.010
1	5	18	2.4	0.658	0.738	0.080
0.5	3	17	3.8	0.668	0.754	0.080
1.0	3	16	2.9	0.670	0.753	0.080
0.9	6	17	4.0	0.672	0.583	−0.080
0.3	3	17	3.4	0.675	0.768	0.090
2.0	5	15	2.0	0.686	0.753	0.060
1.5	4	16	2.0	0.687	0.753	0.060
0.8	6	19	3.0	0.692	0.561	−0.130
0.6	5	16	2.5	0.694	0.743	0.040
0.8	5	20	2.2	0.715	0.708	−0.006
0.9	6	17	2.7	0.720	0.699	−0.020
1.6	6	16	2.2	0.732	0.750	0.010
1.8	3	19	4.0	0.824	0.727	−0.090
2.0	3	15	2.2	0.834	0.753	−0.080
2.0	7	15	3.0	0.834	0.748	−0.080
1.7	7	16	3.0	0.865	0.723	−0.140
1.6	4	16	2.5	0.900	0.753	−0.140
0.4	4	20	2.7	0.935	0.929	−0.005
1.3	4	19	2.0	0.959	0.747	−0.200
0.0	5	15	2.1	0.983	0.948	−0.030
0.8	4	16	2.3	0.986	0.752	−0.230
0.0	5	15	4.0	0.993	0.932	−0.060
1.9	6	18	4.0	0.463	0.496	0.030[a]
2.0	3	19	4.0	0.721	0.730	0.009[a]
1.5	3	18	2.0	0.906	0.753	−0.15[a]

TR transparency ratio
[a] The last three columns are for test date

energy (21) have been reported to influence the stability of nanoemulsions. However, such works are commonly based on one-factor-at-a-time designs which are associated with disadvantages such as inaccurate estimates of the effects. They also study only a small area of the factor space (22). Overall, stability studies to investigate the interactions of the parameters

Table II. The Training Parameters Used with INForm v4.02

Network structure	No. of hidden layers	1
	No. of nodes in hidden layer	3
Back propagation type		Quick Prop
Back propagation parameters	Momentum factor	0.8
	Learning rate	0.7
Targets	Maximum iterations	1000
	MS error	0.0001
	Random seed	10000
Smart stop	Minimum iterations	20
	Test error weighting	0.1
	Iteration overshoot	200
	Auto weight	1
	Smart stop enabled	On
Transfer function	Output	Asymmetric sigmoid
	Hidden layer	Tanh

Table III. The Unseen Data Sets Utilized in ANN Modeling (_n_=1)

Nanoparticle amount, mg/20 cm³	Oil concentration, %_v/v_	Surfactant concentration, %_v/v_	Alcohol concentration, %_v/v_	Result (TR)	Predicted result (TR)	Result error
1.5	7.0	19	2.90	0.446	0.440	−0.0050
0.9	6.5	20	3.75	0.458	0.538	0.0800
0.6	7.0	19	3.10	0.602	0.723	0.1200
2.0	4.0	19	3.50	0.705	0.704	−0.0006
1.4	4.0	17	3.10	0.73	0.752	0.0200
1.3	5.0	18	2.80	0.737	0.729	−0.0070
1.4	3	16	4	0.798	0.753	−0.040
0.7	6	15	3.4	0.862	0.741	−0.1200
1.1	3	17	2.4	0.893	0.753	−0.1300

_TR_ transparency ratio

and avoid the local optima are rare and limited to a work by our group using artificial neural networks (ANNs) (23) and a study by Yuan _et al._ employing response surface methodology (24). Having mentioned that in nanoemulsion preparations, due to the complexity of formulation factors and preparation processes involved (25), evaluation of the effect of independent variables and their simultaneous variation on nanoemulsion properties is not easily obtainable by approaches such as one-factor-at-a-time.

In this study, we employed ANNs as an established method to examine complex and multivariable processes, which have been introduced to deal with non-linear phenomena (26,27). In this study, four variables including concentration of NP, oil, surfactant, and alcohol which may affect the stability of SPIONs-loaded nanoemulsion are chosen to be modeled by ANNs and analyze their effects on the stability of samples.
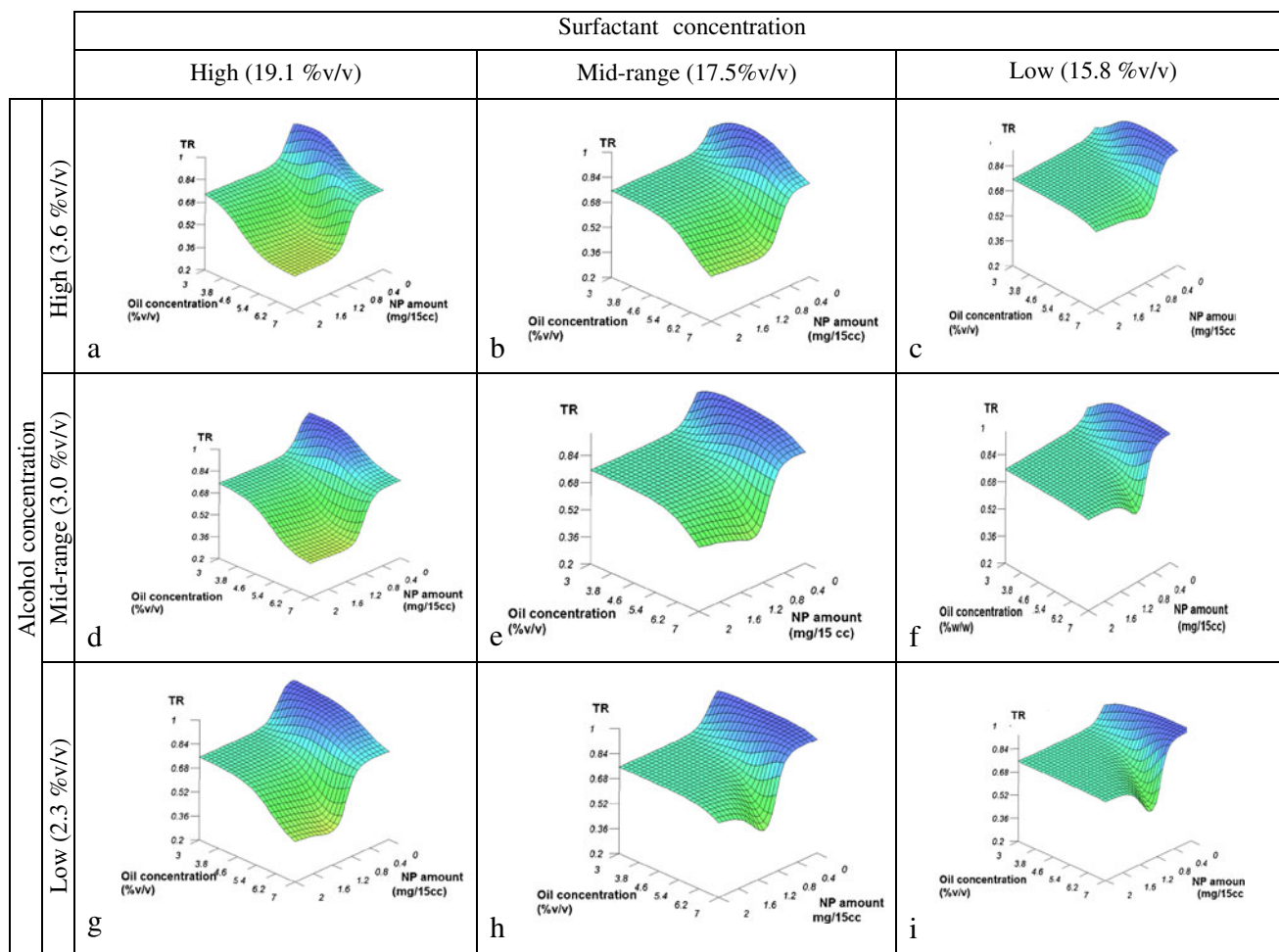

Fig. 1. 3D plot of TR predicted by the ANN model at low, mid range, and high values of concentration of alcohol and surfactant

MATERIALS AND METHODS

Materials

Sweet almond oil was from Sigma-Aldrich (Germany). Tween 80 (polysorbate 80) and alcohol were purchased from Panreac (Spain), and Span 80 was from Merck Chemicals (Germany). The superparamagnetic iron oxide nanoparticles, coated with oleic acid, were synthesized as described previously (28).

Preparation of Samples and Measuring Transparency Ratio

Nanoemulsion samples (20 ml) containing Span 80 and Tween 80 as surfactant, ethanol as co-surfactant, and almond oil as inner phase in deionized water were prepared using UP50H probe sonicator (Hielscher, Germany) by 80% amplitude for 20 min. SPIONs were loaded to the formulation during preparation of the nanoemulsion (18). The transparency of samples (*i.e.*, percentage of transmitted light) using photospectrometer (Novaspec II Pharmacia Biotech,

England) was recorded 30 min and 7 days after preparation. The transparency ratio (TR) (*i.e.*, $\frac{\text{transmitted light after 7 days}}{\text{transmitted light after 30 mins}}$), as an indication of increasing size (29), which may be considered for stability studies (18), was used to investigate the effect of variables on the formulation stability.

Characterization of Nanoemulsion

The appropriate formulation of nanoemulsion, showing the highest stability, was chosen to be characterized in terms of their size, zeta potential, and polydispersity index (PDI) using zeta sizer (Malvern, UK) equipped with the Malvern PCS software (version 1.27).

Data Set

As a commercial ANN software, INForm v4.02 (Intelligensys, UK) was implemented in this study to model the interactions between input variables and their effects on the output. Four variables, namely the concentration of NP, oil,
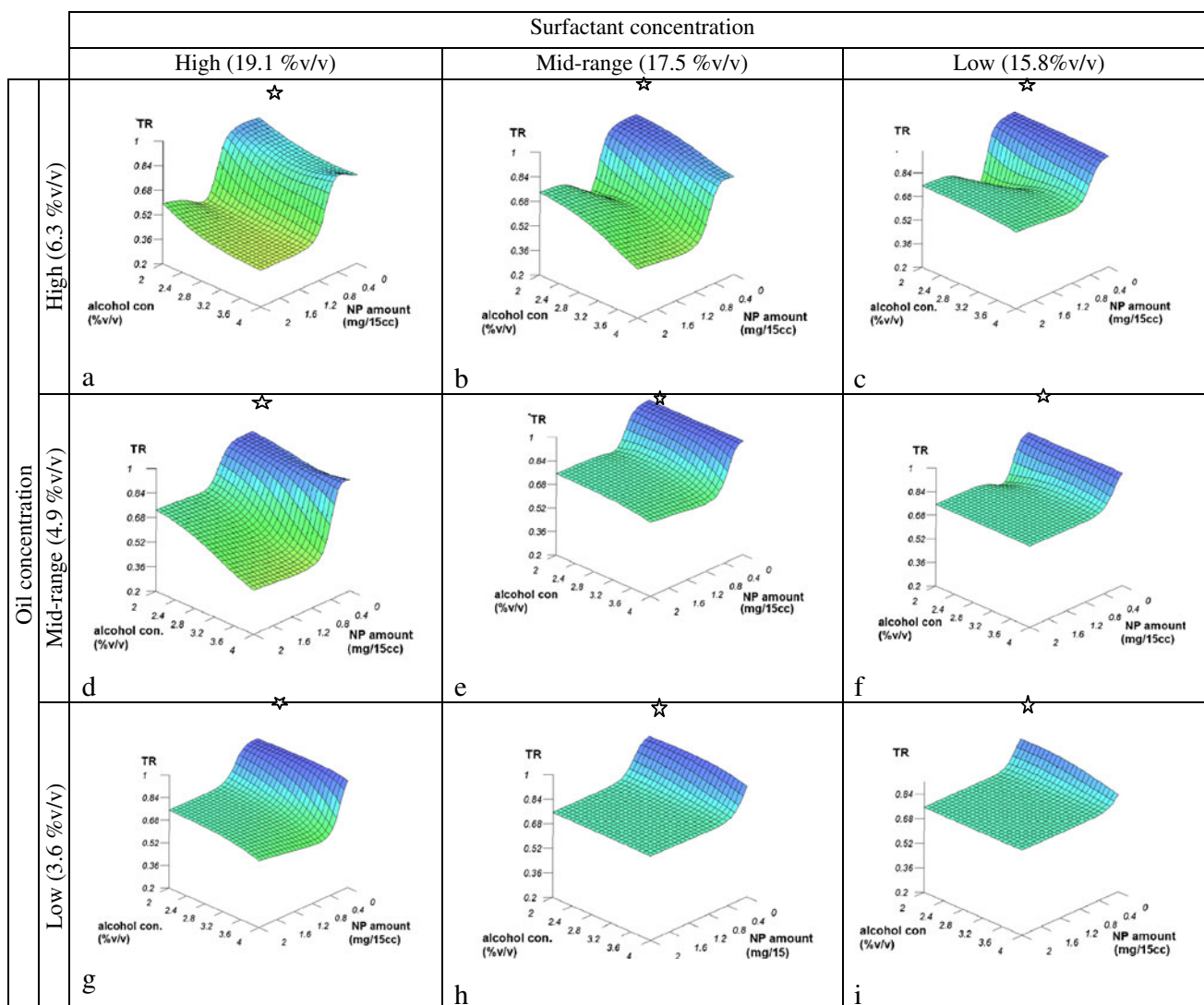

Fig. 2. 3D plot of TR predicted by the ANN model at low, mid range, and high values of concentration of oil and surfactant

surfactant, and alcohol were chosen as inputs of the model, and the TR of samples was considered as the output.

Forty-eight nanoemulsion samples with different values for the four input variables were prepared, and the TR was calculated. These data were then randomly divided into three groups, training, test, and unseen (validation) data. The training set (see Table I) is used to train the network and acquire the relations between inputs and output using training parameters listed in Table II. The test data (see Table I) are employed to prevent overtraining of data. If the overtraining occurs, the correlation coefficient (R^2) (see Eq. 1) obtained for the test data starts to decrease and the training process stops. After training, unseen (validation) data (see Table III) are used to assess the ability of the trained network to predict unseen data. The quality of trained model and its ability to predict the data were evaluated (R^2) for training, test, and validation data from Eq. 1.

$$R^2 = 1 - \frac{\sum_{i=0}^{n}(yi - \grave{y})^2}{\sum_{i=0}^{n}(yi - \bar{y})^2} \tag{1}$$

Where $\grave{y}$ and $\bar{y}$ represent the value predicted by the model and the mean of dependent variables, respectively. An acceptable ANN model needs to have satisfactory R^2 for training and unseen data.

RESULTS

Herein, the decrease in transparency of samples over a certain period was implemented to the model for evaluating the effects of the input variables on the stability of the prepared nanoemulsion.

In our study, to understand the relations between inputs/output variables, a semi-quantitative approach was employed instead of classical sensitivity analysis methodology. In this method, the effects of changing two input variables on the output are studied through visualizing their effects by response surfaces produced by the software, while the remaining two input variables are fixed at three specific values (*i.e.*, low, mid, and high ranges) (30). Following this method, 54 graphs were produced and briefed in Figs. 1, 2, 3, 4, 5, and 6, each representing variation of two inputs and fixing the other two in a 3D graph.
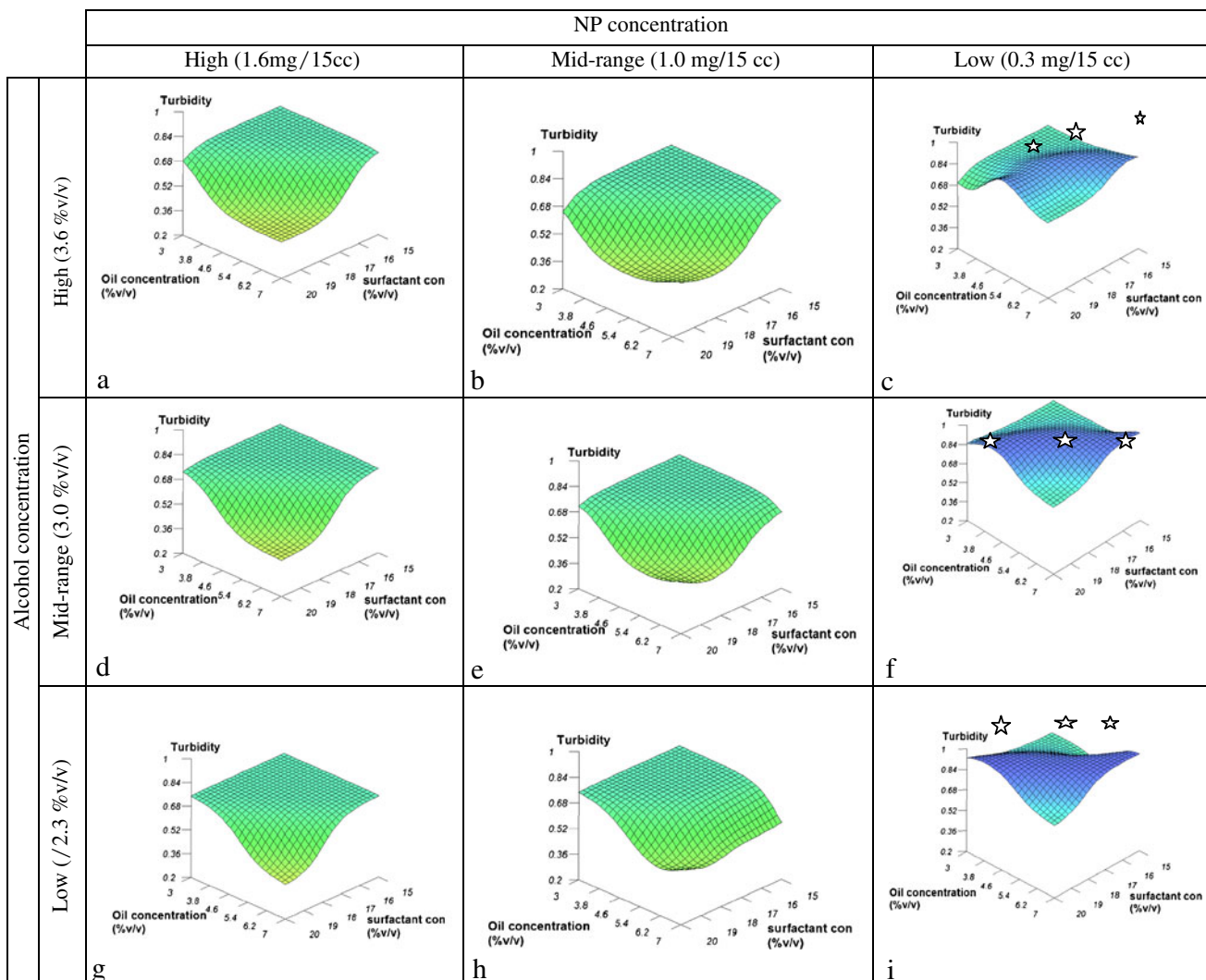

Fig. 3. 3D plot of TR predicted by the ANN model at low, mid range, and high values of concentration of alcohol and NP
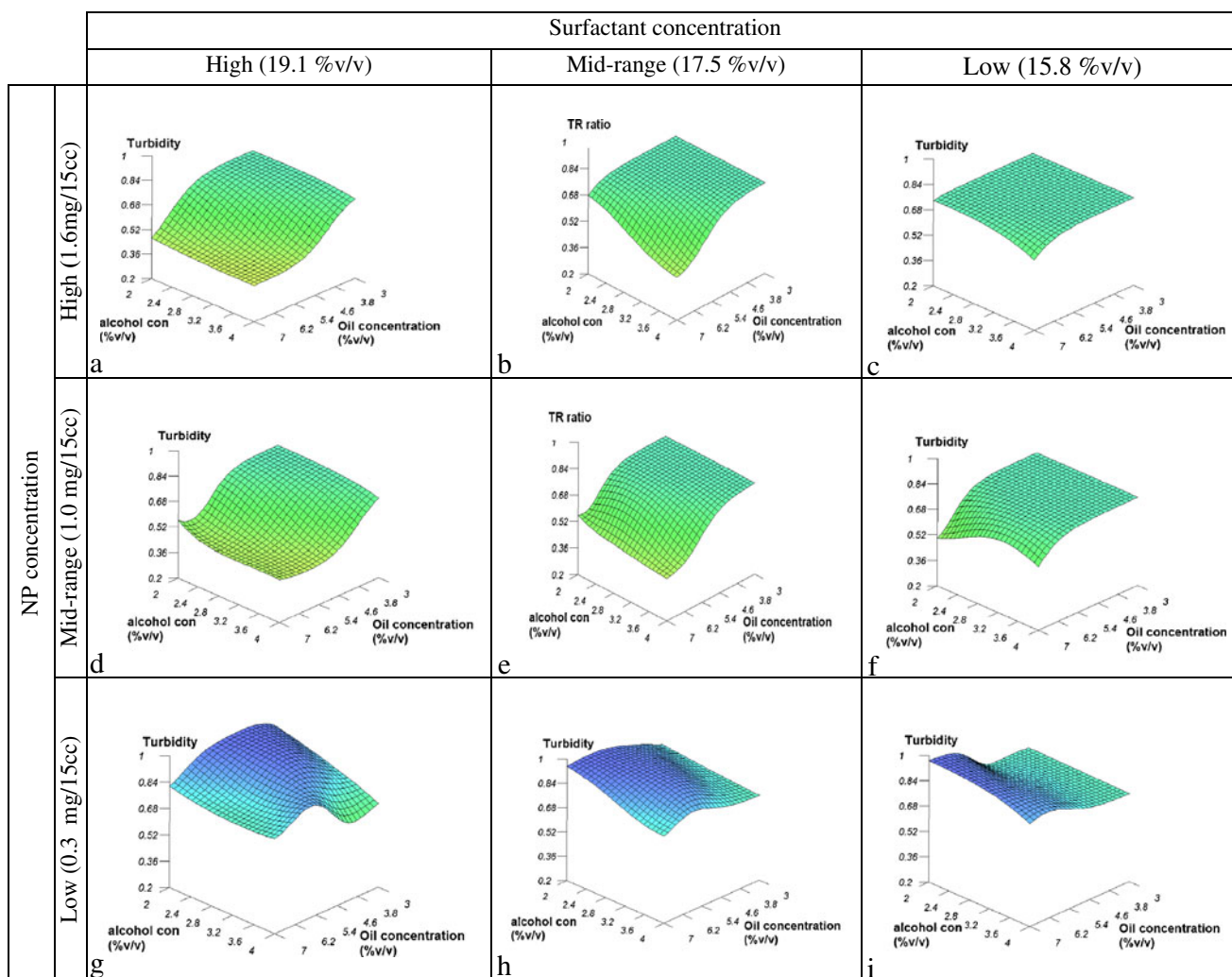
Fig. 4. 3D plot of TR predicted by the ANN model at low, mid range, and high values of concentration of NP and surfactant

In this work, to study the effects of concentration of NP and oil on TR, we first fixed the values for surfactant and alcohol concentration at their low, mid, and high ranges (*i.e.*, 15.8%, 17.4%, and 19.1% *v/v* for surfactant and 2.3%, 3.0%, and 3.6% *v/v* for alcohol). The generated graphs are presented in Fig. 1. Graphs show that, with increasing in the oil concentration, the TR decreases. At low surfactant concentration (15.8% *v/v*) in graphs c, f, and i in Fig. 1, adding oil has less effect on TR in comparison with other graphs. In addition, increasing the amount of NP in general makes the TR ratio smaller. Considering the graphs c, f, and i in Fig. 1, this decrease in the TR ratio is less remarkable when surfactant concentration is low.

In order to study the effects of alcohol and NP concentration on TR, graphs in Fig. 2 were obtained with fixed amount of surfactant and oil at low, mid, and high ranges (*i.e.*, 15.8%, 17.4%, and 19.1% *v/v* for surfactant and 3.6%, 4.9%, and 6.3% *v/v* for oil). Similar to the findings mentioned above, adding NP shows a considerable decrease in TR, ending in a plateau beyond which further increase in NP has no considerable effect. Additionally, the increase in the alcohol concentration makes

the TR smaller with more pronounced effects at high or medium values of oil and/or surfactant concentration. Similarly, the effect of NP concentration on the output is clearer when oil/surfactant values are in high/medium range. The highest TR is observed at minimum level of alcohol (*i.e.*, 2%) with no NP (see asterisk in the graphs). The most stable state in which changes in alcohol and NP have the least effect on TR ratio is seen in graph i of Fig. 2 (*i.e.*, low surfactant and oil).

To evaluate the effects of surfactant and oil concentration on TR, the concentration of NP and alcohol were set at fixed values of low, mid, and high (*i.e.*, 0.3, 1.0, and 1.6 mg/20 cm^3 for NP and 2.3%, 3.0%, and 3.6% *v/v* for alcohol). Considering the details in Fig. 3, when NP concentration is medium or high, TR values close to 1 is not reachable. In this region, both oil and surfactant need to be small to obtain maximum TR value. When NP concentration is small, a temporary increase in the TR is observed, where TR becomes close to 1 in a line, starting from low values of surfactant and high value of oil, moving through mid values of both variables and ending in high value of oil and low value of surfactant (see asterisk in Fig. 3).
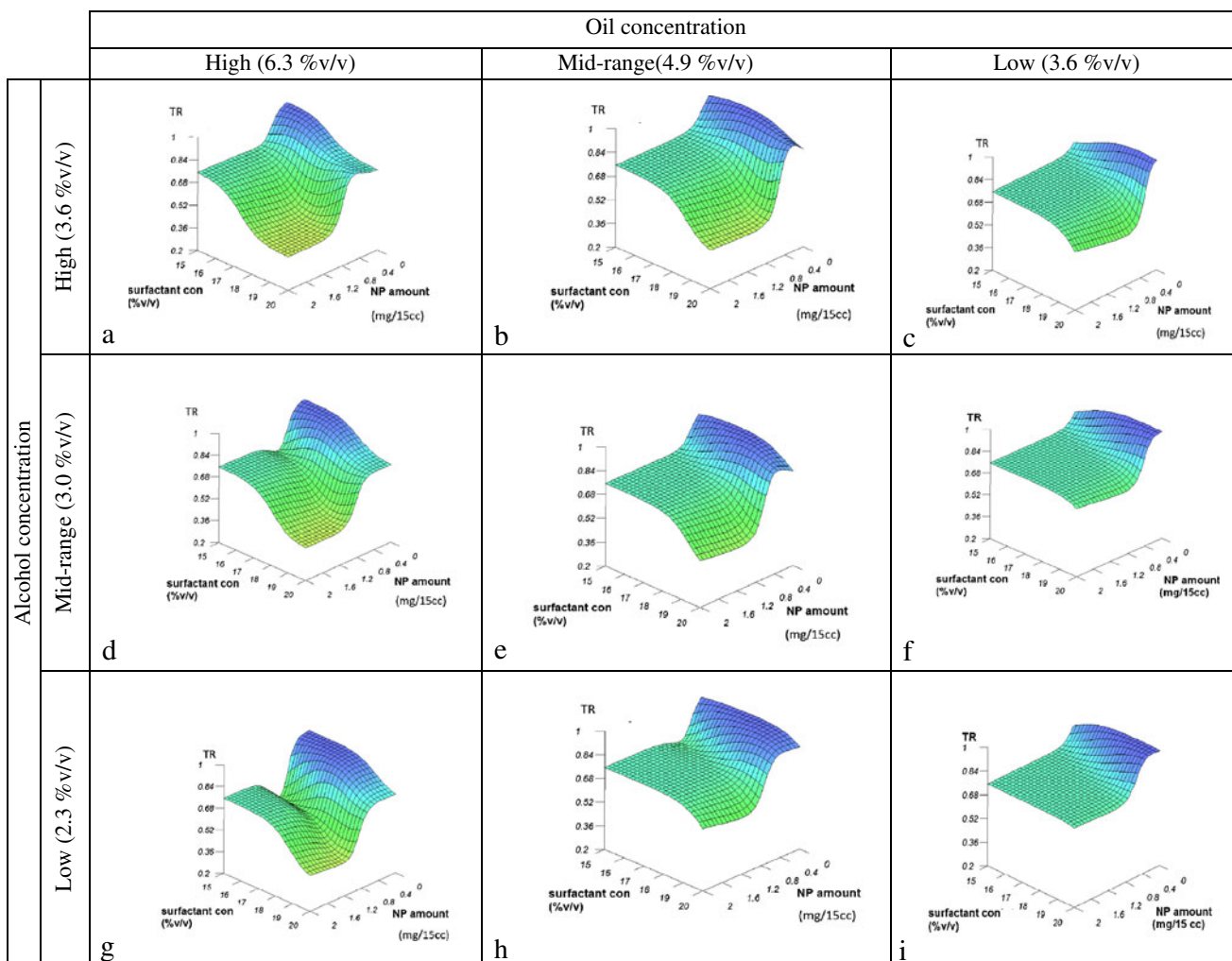
	Oil concentration		
	High (6.3 %v/v)	Mid-range(4.9 %v/v)	Low (3.6 %v/v)

Fig. 5. 3D plot of TR predicted by the ANN model at low, mid range, and high values of concentration of alcohol and oil

From Fig. 4, where the values for surfactant and NP are fixed at low, mid, and high ranges (*i.e.*, 15.8%, 17.4%, and 19.1% *v/v* for surfactant and 0.3, 1.0, and 1.6 mg/20 cm^3 for NP), the effects of oil and alcohol concentration on TR is studied. Details show that when NP concentration is medium or high, adding oil causes a decrease in TR while a different pattern is observed in graphs g, h, and i in Fig. 4 where, at low concentration of NP, adding oil at first increases the TR followed by a decrease in TR. Adding alcohol also shows to have decreasing effect on the TR. This decrease becomes less important in graph c (Fig. 4), where surfactant is low and NP is high.

Considering Figs. 5 and 6, which illustrate the effects of NP and surfactant concentration as well as surfactant and alcohol concentration on the TR ratio, respectively, the following results may be confirmed:

– Elevating the NP concentration shows considerable decrease in the TR ratio, ending in a plateau. Adding NP at low value of oil shows the least effect on TR ratio.
– Increasing concentration of surfactant after a threshold leads to considerable decrease in the ratio, especially when oil concentration is increased simultaneously.

– Adding alcohol leads to decrease in the TR; this increase is more obvious when surfactant concentration is elevated.

Sample Characterization Results

Analyzing the response surfaces produced by the model, the optimum sample with probably highest stability was suggested to contain 15% *v/v* surfactant, 5% *v/v* oil, 2.5% *v/v* co-surfactant, and 1.5 mg/15 cm^3 SPION. The mean droplet size and zeta potential of the optimum sample revealed to be 38.6 and 0.3 nm, respectively, with PDI 0.154, indicating a monodispersed preparation. In an attempt to study the long-term physical stability of the sample, a preliminary study was performed at room temperature (22°C±2°C). No evidence of phase separation was observed for minimum 1.5 years.

DISCUSSION

To estimate the stability of nanoemulsions, several methods have been proposed in the literature including heating–cooling and freeze–thaw cycles (31), centrifugation (32), Turbiscan analysis (33), and microscopic observation of phase separation (34). In this work, we used the decrease in the
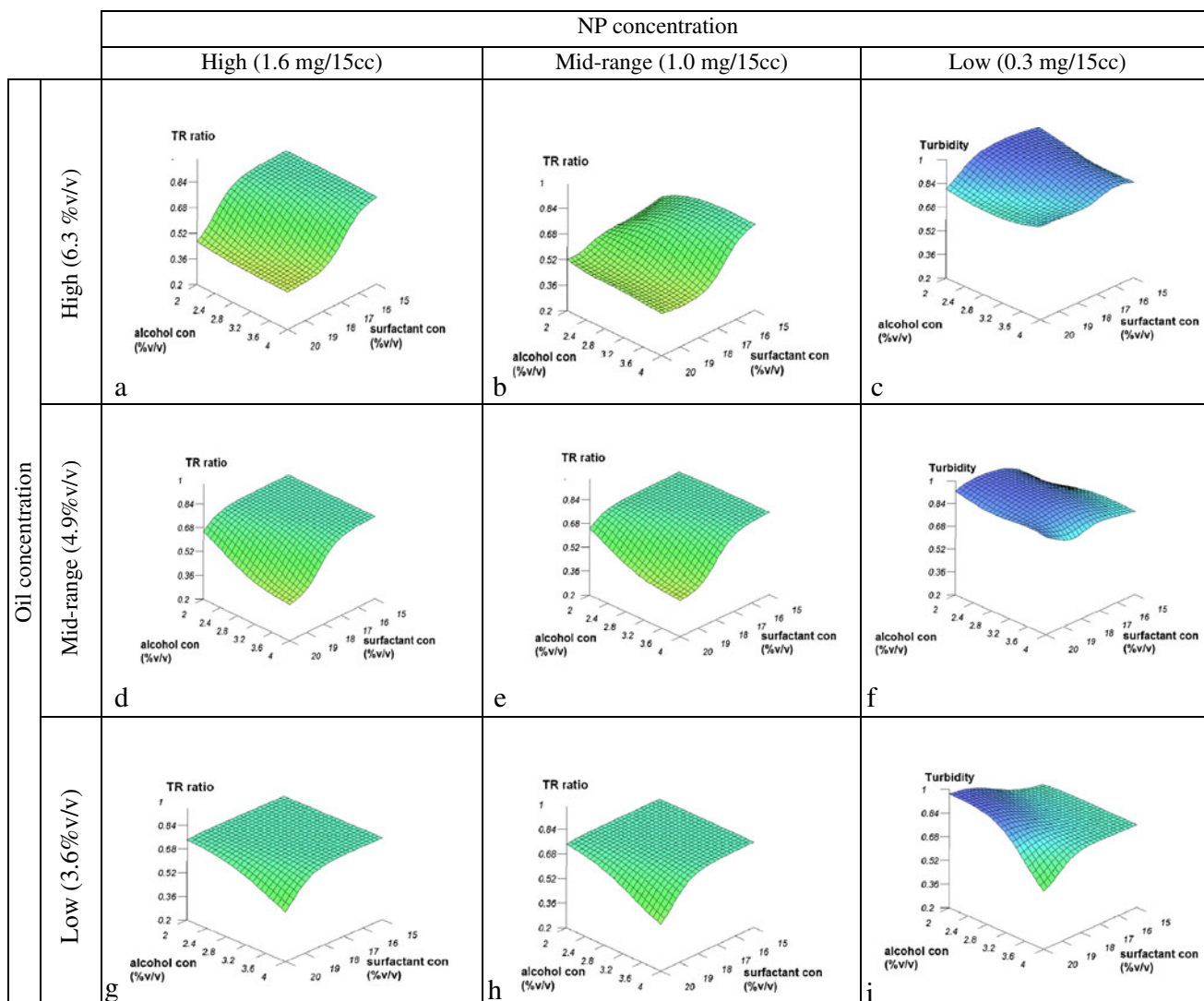
Fig. 6. 3D plot of TR predicted by the ANNs model at low, mid range, and high values of concentration of oil and NP

transparency of nanoemulsion as an indication of increasing size (29) which can be considered to estimate the stability of nanoemulsion (18).

The model in our study showed that an optimum concentration of surfactant leads to the most stable state and exceeding beyond this concentration would not improve the stability anymore. This is in agreement with the study of Barad *et al.* (35) which shows that increasing the surfactant more than an optimum amount will not improve the stability. Additionally, further increases of the surfactant concentration in our work resulted in instability of the preparation. This could be due to several reasons:

– Brownian motion increases as a result of smaller size arising from increase in surfactant concentration. The increase in Brownian motions is then followed by increase in Ostwald ripening.
– The number of micelles increases, which results in further collisions between micelles. This ends up in increasing the micelles size.

– At higher concentrations of surfactant, the surfactant aggregations with lamellar liquid crystalline structure would occur instead of micelles, making the preparation more turbid (36).

In our study, adding alcohol more than a minimum amount (about 2.2% *v/v*) shows a decrease in TR. This finding agrees with studies indicating the importance of co-surfactant concentration and proper ratio of co-surfactant to surfactant (37). Alcohol as a co-surfactant seems to position in the interfacial film with its –OH group lying among hydrophilic parts of surfactant and neighboring water molecules, while its hydrophobic chain stretches towards hydrophobic chains of surfactant. Nevertheless, excess amount of alcohol molecules replaces the surfactant molecules, thus, making the nanoemulsion droplets less stable. Furthermore, hydrogen binding between OH group of alcohol and polar chains of surfactant can occur, which lowers the fluidity of the interfacial film, making the preparation less stable (38). Additionally, alcohol molecules may enter the inner phase, which causes the expansion of the interfacial film, leading to size increase and instability (39).

Our findings also showed that going from low to high values of oil decreases the TR, most probably as a result of size increasing of the hydrophobic core and the whole particle (40,41). It can be argued that loading more oil molecules into the nanoemulsion particles makes them more polydispersed which pushes the system towards Oswald ripening (42). Similarly, adding NP shows a decrease on the TR which can be due to the size increasing. Subsequently, by increasing the core size, the interfacial film expands and causes elevating in TR ratio. Moreover, the obtained model indicates that in high amount of NP and low concentration of oil, the nanoemulsion maintains its TR in wide variation of other variables. This might be from proper interactions of oleic acid molecules— which are coating NP—with almond oil (of which 62% comprises of oleic acid). Such interactions may lead to more packed structure.

CONCLUSION

In a system with several components, finding relations between variables, which affect the system's property, is a complicated task to do. In this study, using ANNs, a model has been developed to provide an appropriate insight into factors affecting the decrease in the transparency of nanoemulsion as an indication of stability. Using response surfaces generated from the ANNs model, contribution of factors affecting the stability of nanoemulsion is observed. The model indicated that all four input variables, namely, concentration of oil, surfactant, co-surfactant, and loaded nanoparticle have reverse relation with the stability of preparation. The most stable system is achieved at low surfactant concentration ($\sim$15.8%v/v), low range of oil ($\sim$3.6%v/v), low amount of NP ($\sim$0.3 mg/15 cm^3), and low range of alcohol ($\sim$2.3%v/v).

ACKNOWLEDGMENT

REFERENCES

1. Pankhurst QA, Thanh NKT, Jones SK, Dobson J. Progress in applications of magnetic nanoparticles in biomedicine. J Phys D Appl Phys. 2009;42:224001.
2. Berry CC, Curtis ASG. Functionalisation of magnetic nanoparticles for applications in biomedicine. J Phys D Appl Phys. 2003;36:R198.
3. Gupta AK, Gupta M. Synthesis and surface engineering of iron oxide nanoparticles for biomedical applications. Biomaterials. 2005;26(18):3995–4021.
4. Olsvik O, Popovic T, Skjerve E, Cudjoe KS, Hornes E, Ugelstad J, *et al*. Magnetic separation techniques in diagnostic microbiology. Clin Microbiol Rev. 1994;7(1):43.
5. Jarzyna PA, Skajaa T, Gianella A, Cormode DP, Samber DD, Dickson SD, *et al*. Iron oxide core oil-in-water emulsions as a multifunctional nanoparticle platform for tumor targeting and imaging. Biomaterials. 2009;30(36):6947–54.
6. Fornara A. Multifunctional nanomaterials for diagnostic and therapeutic applications. KTH, Stockholm, Sweden. 2010.
7. Fukuchi K, Tomoyasu S, Tsuruoka N, Gomi K. Iron deprivation-induced apoptosis in HL-60 cells. FEBS Lett. 1994;350(1):139–42.
8. Porreca E, Ucchino S, Di Febbo C, Di Bartolomeo N, Angelucci D, Napolitano AM, *et al*. Antiproliferative effect of desferrioxamine on vascular smooth muscle cells *in vitro* and *in vivo*. Arterioscler Thromb Vasc Biol. 1994;14(2):299–304.
9. Halliwell B, Gutteridge JM. Oxygen toxicity, oxygen radicals, transition metals and disease. Biochem J. 1984;219(1):1.
10. Emerit J, Beaumont C, Trivin F. Iron metabolism, free radicals, and oxidative injury. Biomed Pharmacother. 2001;55(6):333–9.
11. Arbab AS, Bashaw LA, Miller BR, Jordan EK, Lewis BK, Kalish H, *et al*. Characterization of biophysical and metabolic properties of cells labeled with superparamagnetic iron oxide nanoparticles and transfection agent for cellular MR imaging. Radiology. 2003;229(3):838.
12. Laurent S, Forge D, Port M, Roch A, Robic C, Vander Elst L, *et al*. Magnetic iron oxide nanoparticles: synthesis, stabilization, vectorization, physicochemical characterizations, and biological applications. Chem Rev. 2008;108(6):2064–110.
13. Sun C, Lee JSH, Zhang M. Magnetic nanoparticles in MR imaging and drug delivery. Adv Drug Deliv Rev. 2008;60(11):1252–65.
14. Sutton D, Nasongkla N, Blanco E, Gao J. Functionalized micellar systems for cancer targeted drug delivery. Pharm Res. 2007;24 (6):1029–46.
15. Varanda LC, Junior MJ, BeckJunior W. Magnetic and multifunctional magnetic nanoparticles in nanomedicine: challenges and trends in synthesis and surface engineering for diagnostic and therapy applications. In: Laskovski AN, editor. Biomedical Engineering, Trends in Materials Science: InTech; 2011.
16. Yang J, Lee CH, Ko HJ, Suh JS, Yoon HG, Lee K, *et al*. Multifunctional magneto-polymeric nanohybrids for targeted detection and synergistic therapeutic effects on breast cancer. Angew Chem Int Ed Engl. 2007;46(46):8836–9.
17. Von Rybinski W, Guckenbiehl B, Tesmann H. Influence of co-surfactants on microemulsions with alkyl polyglycosides. Colloids Surf, A Physicochem Eng Asp. 1998;142(2–3):333–42.
18. Amani A, York P, Chrystyn H, Clark BJ. Factors affecting the stability of nanoemulsions—use of artificial neural networks. Pharm Res. 2010;27(1):37–45.
19. Wooster TJ, Golding M, Sanguansri P. Impact of oil type on nanoemulsion formation and Ostwald ripening stability. Langmuir. 2008;24(22):12758–65.
20. He W, Tan Y, Tian Z, Chen L, Hu F, Wu W. Food protein-stabilized nanoemulsions as potential delivery systems for poorly water-soluble drugs: preparation, *in vitro* characterization, and pharmacokinetics in rats. Int J Nanomedicine. 2011;6:521-533.
21. Kentish S, Wooster TJ, Ashokkumar M, Balachandran S, Mawson R, Simons L. The use of ultrasonics for nanoemulsion preparation. Innov Food Sci Emerg Tech. 2008;9(2):170–5.
22. Czitrom V. One-factor-at-a-time *versus* designed experiments. Am Stat. 1999;53:126–131.
23. Amani A, York P, Chrystyn H, Clark BJ. Factors affecting the stability of nanoemulsions—use of artificial neural networks. Pharm Res. 2010;27(1):37–45.
24. Yuan Y, Gao Y, Mao L, Zhao J. Optimisation of conditions for the preparation of [beta]-carotene nanoemulsions using response surface methodology. Food Chem. 2008;107(3):1300–6.
25. Amani A, Mohammadyani D. Artificial neural networks: applications in nanotechnology. In: Hui C-L, editor. Artificial neural networks—application. Rijeka: INTECH; 2011. Available from: http://www.intechopen.com/articles/show/title/artificial-neural-networks-applications-in-nanotechnology.
26. Bourquin J, Schmidli H, van Hoogevest P, Leuenberger H. Comparison of artificial neural networks (ANN) with classical modelling techniques using different experimental designs and data from a galenical study on a solid dosage form. Eur J Pharm Sci. 1998;6(4):287–300.
27. Sathe PM, Venitz J. Comparison of neural network and multiple linear regression as dissolution predictors. Drug Dev Ind Pharm. 2003;29(3):349–55.
28. Faridi-Majidi R, Sharifi-Sanjani N, Agend F. Encapsulation of magnetic nanoparticles with polystyrene via emulsifier-free miniemulsion polymerization. Thin Solid Films. 2006;515 (1):368–74.
29. Liu J, Wang X, Tan H, Liu H, Wang Y, Chen R, *et al*. Effect of heparin-superoxide dismutase on I^3-radiation induced DNA damage *in vitro* and *in vivo*. Drug Discov Ther. 2010;4(5):355–61.
30. Aghajani M, Shahverdi AR, Rezayat SM, Amini MA, Amani A. Preparation and optimization of acetaminophen nanosuspension

through nanoprecipitation using microfluidic devices—an artificial neural networks study. Pharm Dev Technol. 2012 (in press).

31. Shafiq S, Shakeel F, Talegaonkar S, Ahmad FJ, Khar RK, Ali M. Development and bioavailability assessment of ramipril nanoemulsion formulation. Eur J Pharm Biopharm. 2007;66(2):227–43.

32. Moreno MA, Ballesteros MP, Frutos P. Lecithin-based oil-in-water microemulsions for parenteral use: pseudoternary phase diagrams, characterization and toxicity studies. J Pharm Sci. 2003;92(7):1428–37.

33. Mao L, Xu D, Yang J, Yuan F, Gao Y, Zhao J. Effects of small and large molecule emulsifiers on the characteristics of b-carotene nanoemulsions prepared by high pressure homogenization. Food Technology and Biotechnology. 2009;47:336-342

34. Tcholakova S, Denkov ND, Danner T. Role of surfactant type and concentration for the mean drop size during emulsification in turbulent flow. Langmuir. 2004;20(18):7444–58.

35. Barad JM, Chakraborty M, Bart HJ. Formation and stability study of nano-emulsions: BTX-separation. Open Chem Eng J. 2009;3:33–40.

36. Izquierdo P, Esquena J, Tadros TF, Dederen C, Garcia MJ, Azemar N, et al. Formation and stability of nano-emulsions prepared using the phase inversion temperature method. Langmuir. 2002;18(1):26–30.

37. Gao ZG, Choi HG, Shin HJ, Park KM, Lim SJ, Hwang KJ, et al. Physicochemical characterization and evaluation of a microemulsion system for oral delivery of cyclosporin A. Int J Pharm. 1998;161(1):75–86.

38. Resende KX, Correa MA, Oliveira AG, Scarpa MV. Effect of cosurfactant on the supramolecular structure and physicochemical properties of non-ionic biocompatible microemulsions. Rev Bras Cienc Farm. 2008;44(1):35–42.

39. Xi J, Chang Q, Chan CK, Meng ZY, Wang GN, Sun JB, et al. Formulation development and bioavailability evaluation of a self-nanoemulsified drug delivery system of oleanolic acid. AAPS PharmSciTech. 2009;10(1):172–82.

40. Sevcikova P, Vltavska P, Kasparkova V, Krejci J. Formation, characterization and stability of nanoemulsions prepared by phase inversion. Proceedings of the 13th WSEAS international conference on Mathematical and computational methods in science and engineering. 2011:132–7.

41. Sakeena MHF, Elrashid SM, Munavvar AS, Azmin MN. Effects of oil and drug concentrations on droplets size of palm oil esters (POEs) nanoemulsion. J Oleo Sci. 2011;60(4):155–8.

42. He W, Tan Y, Tian Z, Chen L, Hu F, Wu W. Food protein-stabilized nanoemulsions as potential delivery systems for poorly water-soluble drugs: preparation, in vitro characterization, and pharmacokinetics in rats. Int J Nanomedicine. 2011;6:521.